CHEMISTRY
A European Journal

A Journal of ChemPubSoc Europe

Title: The influence of alkali metal ions on the stability and reactivity of chromium(III) superoxide moieties spanned by siloxide ligands

Authors: Christian Limberg, Marie-Louise Wind, Santina Hoof, Christian Herwig, and Beatrice Braun-Cula

To be cited as: *Chem. Eur. J.* 10.1002/chem.201900236

Link to VoR: http://dx.doi.org/10.1002/chem.201900236

Supported by ACES

WILEY-VCH

Chemistry - A European Journal 10.1002/chem.201900236

The influence of alkali metal ions on the stability and reactivity of chromium(III) superoxide moieties spanned by siloxide ligands

Marie-Louise Wind, Santina Hoof, Christian Herwig, Beatrice Braun-Cula and Christian Limberg*[a]

Abstract: In recent years it has become clear that the presence of *redox-inactive* Lewis acidic metal ions can decisively influence the reactivity of metal-dioxygen moieties formed in the course of O_2 activation, in molecular complexes and metalloenzymes. Superoxide species are often formed as the primary intermediates but they are mostly too unstable for a thorough investigation. We have found an access to a series of chromium(III) superoxide complexes $[L_2Cr]M_2O_2(THF)_y$ ($L = {}^{-}OSiPh_2OSiPh_2O^{-}$, $M^+ = Li^+$, Na^+, K^+ and y = 4, 5), which can be spectroscopically studied, partly also crystallized at low temperatures and which differ only in the two Lewis acidic alkali metal counterions M^+ incorporated in the structures. It is shown here that the nature of M^+ sensitively determines its interaction with the superoxide ligand formed and that this interaction in turn has a significant influence on the stability and reactivity of these complexes towards substrates with OH groups. Furthermore, we are able to show that stability and reactivity are also highly solvent dependent (THF vs. nitriles), as donor solvents coordinate to the alkali metal ions and thus also influence their interaction with the superoxide moiety. Altogether the results obtained provide a comprehensive and detailed picture concerning the correlation between spectroscopic properties, structure and behavior of such superoxides, that may be exemplary for other systems.

Introduction

The binding and activation of molecular oxygen represents a key step in many industrial and biological processes, where organic substrates are oxidized and thus converted into value-added products. At first glance it may seem surprising that O_2 activation is necessary considering the potential reactivity of O_2 from a thermodynamic standpoint. However, there is a kinetic barrier inherent to its reactions with singlet molecules, which has to be overcome, and this is typically achieved by partnering O_2 with species that can undergo single electron transfers or that possess unpaired electrons, such as redox-active metal ions.[1] Dioxygen-activating compounds, both in research laboratories and in nature, therefore often contain, for instance, iron, copper, molybdenum or chromium ions.[2] Within the last decade it became obvious, though, that also redox-inactive metal ions, if simultaneously present, can play an important role in the O_2 activation processes due to their Lewis acidic properties.[3] Investigations on the interaction of Lewis acids with reactive metal/dioxygen systems and metal oxo complexes have thus become a lively and emerging area within the field of oxidation chemistry and the number of studies, where Lewis acidic metal ions are added deliberately to such systems is continuously increasing.[4] The results obtained indicated that it is possible to significantly increase the stability of short-lived metal oxo intermediates by adding Lewis acids. For instance, in the presence of metal ions such as Sc^{III}, Zn^{II} or Ce^{III} the intermediate formed in a reaction of a cobalt complex with O_2 could be stabilized, which allowed a spectroscopic analysis of the transient species.[5,6] In contrast to this, it could also be shown that the addition of Lewis acids such as Sc^{III}, Y^{III}, Lu^{III} or La^{III} enhances the reactivity of a non-heme iron(III) peroxo complex in single electron transfer and electrophilic reactions.[7] Moreover, Ohkubo *et al.* observed that the rate of the one-electron conversion of O_2 to a superoxide ion is directly correlated with the Lewis acidities of added redox-inactive metal ions, underlining that these indeed play an important role in dioxygen activation.[8]

We have recently investigated the mononuclear complex $[L_2Cr]Li_2(THF)_4$ (**1**) (Scheme 1) formed via the reaction of the disilanol, 1,1,3,3-tetraphenylsilan-1,3-diol (LH_2), with $^{n}BuLi$ and $CrCl_2$. **1** was found to readily react with dioxygen forming the chromium(III) superoxide complex $[L_2Cr]Li_2O_2(THF)_5$ (**2**), which could be crystallized at low temperatures.[9] In **2** one Li^+ ion is lifted out of the CrO_4 plane, so that an electrostatic interaction between the distal O atom of the superoxide ligand and the Lewis acid Li^+ occurs (Scheme 1). The interaction leads evidently to a stabilization of the chromium(III) superoxide unit and has thus allowed us to stop the reaction of **1** with O_2 directly after the primary O_2 activation step.[9] Although complex **2** is intrinsically quite unstable in THF,[9] it reacts only slowly with organic substrates such as 2,6-di-*tert*-butyl-4-methoxyphenol, This stands in contrast to other reported mononuclear chromium(III) superoxide complexes (mostly in an N-donor surrounding and without coordinating Lewis acids), which not only display a higher stability but also readily react with organic substrates.[10] The lower reactivity of $[L_2Cr]Li_2O_2(THF)_5$ (**2**) may be rationalized by either the stabilizing interaction of the superoxide moiety with the lithium cation or the shielding of the Cr–OO unit by the phenyl residues of the two disiloxide ligands. Here we now present results of an investigation concerning the influence of M^+ ($M^+ = Li^+$, Na^+, K^+) on the structure, reactivity and stability of the superoxide moieties in complexes of the type $[L_2Cr]M_2O_2$.

---

[a] Dipl. Chem. M.-L. Wind, M. Sc. S. Hoof, Dr. B. Braun-Cula, Dr. C. Herwig, Prof. C. Limberg
Humboldt-Universität zu Berlin
Department of Chemistry
Brook-Taylor-Strasse 2, 12489 Berlin, Germany
E-mail: Christian.limberg@chemie.hu-berlin.de

Supporting information for this article is given via a link at the end of the document.

10.1002/chem.201900236

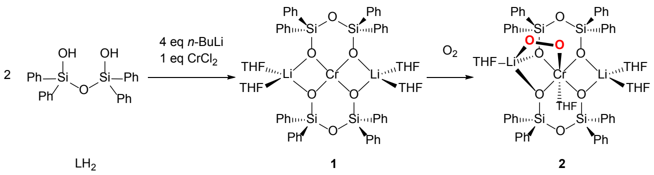

Scheme 1: Synthesis of compounds **1** and **2**.

Results and Discussion

Synthesis of the chromium(II) precursor compounds $[L_2Cr]M_2$ ($M = Na^+$, K^+) To determine to what extent the Lewis acidic cation Li^+ influences the stability and the reactivity of the chromium superoxide unit, the synthesis of chromium(II) complexes analogous to **1** with different alkali metal cations, M^+, was inevitable. $[L_2Cr]Na_2(THF)_4$ (**3**), which had been described previously by Motevalli *et al.* [11], was prepared by using NaO^tBu as a base to deprotonate LH_2. After addition of $CrCl_2$ and work-up, **3** could be isolated in form of orange crystals. The corresponding potassium complex $[L_2Cr]K_2(THF)_4$ (**4**) was synthesized in a similar way. By layering a concentrated THF solution of **4** with hexane orange crystals suitable for X-ray diffraction analysis could be grown. The structure determined corresponds to a coordination polymer, **4'**, which is derived from **4** formally by elimination of two THF molecules (Fig. 1).

This leads to molecular units of **4** being linked by moieties, in which the THF ligands at the K^+ ions are missing and the potassium ions interact electrostatically with the phenyl rings of the neighboring molecules, so that a chain with the sequence $AB(AB)_n$ is formed. In both units A and B the two disiloxide ligands provide an almost perfectly square-planar coordination sphere for the chromium(II) ions (Fig. 1). A comparison of the structural parameters of the chromium(II) compounds, **1**, **3** and **4'**, shows that the nature of the alkali metal does not have a major influence on the Si–O or the O–Cr bond lengths of the chromium(II) compounds.

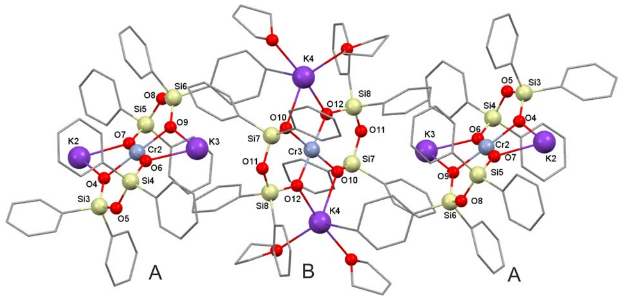

Figure 1: Polymeric structure of compound **4'**. Hydrogen atoms are omitted for clarity. Selected bond lengths in Å and angles in°: **A** O4–Cr2 2.0225(10), O6–Cr2 2.0053(10), O9–Cr2 2.0176(10), O7–Cr2 1.9977(10), Cr2-O9-K3 98.93(4), Cr2-O4-K2 98.12(4), Cr2-O6-K3 100.08(4), Cr2-O7-K2 102.56(4), Si3-O4-K2 130.75(5), Si4-O6-K3 125.21(5), **B** O10–Cr3 2.0108(10), O10–K4 2.6129(10), O12–Cr3 1.9893(9), O12–K4 2.5694(10), Cr3–K4 3.6166(4), Cr3-O12-K4 104.27(4), Cr3-O10-K4 102.13(4), Si7-O10-K4 119.19(5).

Influence of the alkali metal ions on the spectroscopic and structural parameters of the respective chromium(III) superoxides To test the reactivity of **3** and **4** towards dioxygen a 2 mM THF solution of the respective complexes was prepared, cooled to –80 °C and then exposed to an excess of molecular oxygen. The reactions were monitored via UV/vis spectroscopy. After completion of the reaction of $[L_2Cr]Na_2(THF)_4$ (**3**) with dioxygen, the recorded UV/vis spectrum of the chromium dioxygen adduct showed two distinctive absorption bands at 319 nm and at 712 nm as well as a weak band at 508 nm (Fig. 2 B). The UV/vis spectrum after treatment of the corresponding potassium complex with O_2 exhibits absorption bands at 325 nm as well as at 735 nm (Fig. 2 C). This is in contrast to what was found for the chromium superoxide complex **2** with lithium as a counter ion: **2** shows absorption bands not only at around 300 and 700 nm (concretely at 310 nm and 691 nm) but also at 507 nm and 881 nm (Fig. 2 A). The bathochromic shift of the bands in the region of 300 and 700 nm increasing from **1**+O_2 to **3**+O_2 and **4**+O_2 can be ascribed to the different nature of M^+.[12,13]

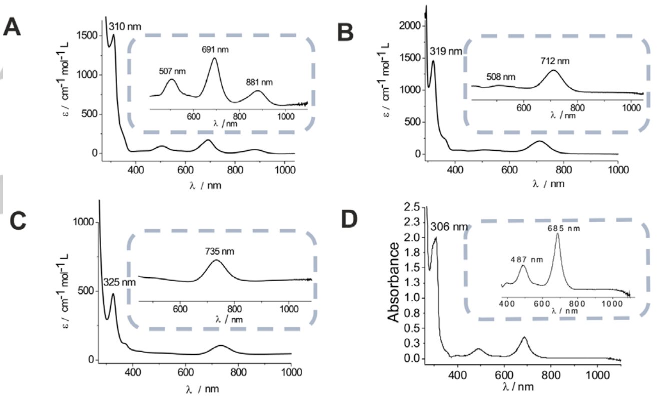

Figure 2: Absorption spectra recorded for a 2 mM solution of A) **1** after treatment with O_2: λ_{max} (ε in cm^{-1} mol^{-1} L) = 310, 507, 691, 881 nm, B) **2** after treatment with O_2: λ_{max} (ε in cm^{-1} mol^{-1} L) = 319 (1460), 508 (72), 712 (222) nm, C) **4** after treatment with O_2: λ_{max} (ε in cm^{-1} mol^{-1} L) = 325 (484), 735 (112) nm. D) Absorption spectra of **6**·EtCN re-dissolved in EtCN: λ_{max} = 306, 487, 685 nm.

For the reduced number of absorption bands two different explanations are conceivable: 1) a different chromium dioxygen adduct or 2) a chromium(III) superoxide complex with a changed M^+/O_2 interaction was formed.[14] While Raman data for **2** dissolved in MeCN have been reported previously[9] (and are reported here for the EtCN solvate **6** (see below)) measurements on the products **3**+O_2 and **4**+O_2 were unsuccessful, due to the light sensitivity of the complexes. However, single crystals of the product formed in the reaction of **3** with O_2 could be grown and prepared at –80 °C. X-ray diffraction analysis revealed that **3** upon addition of dioxygen forms – similar to **1** – a chromium(III) complex with an end-on bound superoxide ligand $[L_2Cr]Na_2O_2(THF)_5$·THF, **5**·THF (Fig. 3). Due to a slight pseudosymmetry towards *Pbca* there are two molecules with similar bond lengths present in the unit cell. The arithmetic mean of the O–O bond lengths of the two molecules (O7–O8 1.334(7) and O20–O21 1.324(7) Å) present in the unit cell, namely 1.33 Å, is almost identical to the one determined for

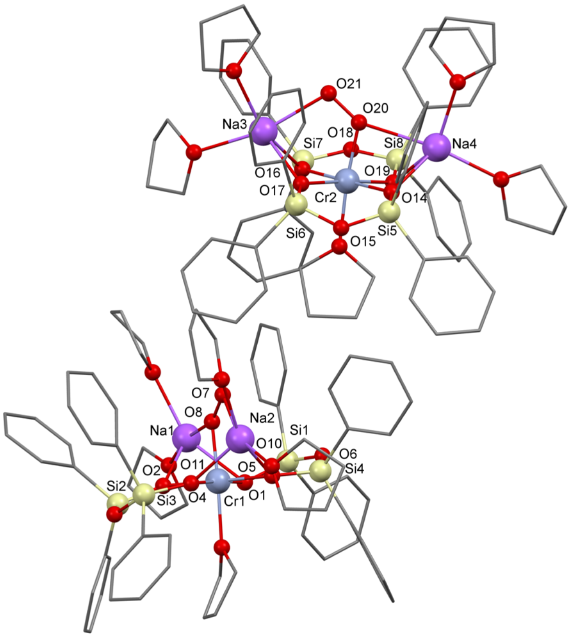

Figure 3: Molecular structure of **5**. For clarity hydrogen atoms are omitted. Selected bond lengths in Å and angles in °: Cr1–O8 1.881(6), Cr1–O4 1.954(5), Cr1–O5 1.958(5), Cr1–O1 1.976(5), Cr1–O2 1.977(5), Cr1–Na1 3.016(3), Cr1–Na2 3.091(3), Na1–O8 2.500(6), Na2–O4 2.279(6), O7–O8 1.334(7), Cr2–O20 1.888(6), Cr2–O16 1.951(5), Cr2–O17 1.964(5), Cr2–O19 1.971(5), Cr2–O14 1.981(5), Cr2–Na4 3.020(3), Cr2–Na3 3.072(3), Na3–O21 2.373(6), Na4–O20 2.562(6), O20–O21 1.324(7), O7-O8-Cr1 121.6(4), O8-O7-Na2 106.1(4), O4-Na2-O7 82.2(2), O5-Na2-O7 77.4(2), O4-Cr1-Na1 128.50(17), O8-O7-Na2 106.1(4), O7-O8-Cr1 121.6(4), O7-O8-Na1 152.6(5), Cr1-O8-Na1 85.8(2), O20-Cr2-Na4 57.53(17), O20-O21-Na3 106.1(4), O21-O20-Cr2 122.1(4), O21-O20-Na4 153.8(5).

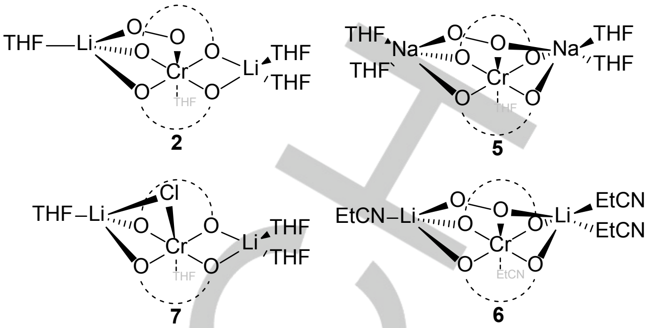

Chart 1: Depiction of the cores of compounds **2**, **5**, **6** and **7**.

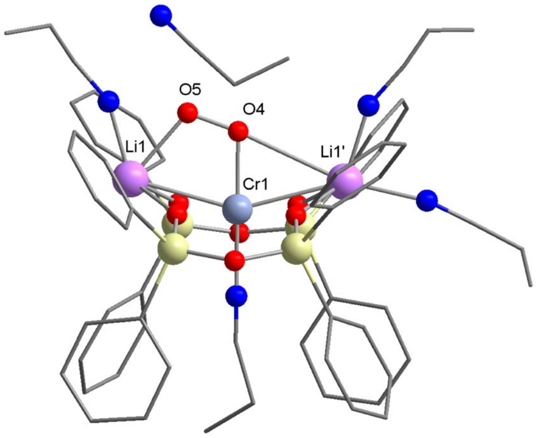

Figure 4: Molecular structure of **6**·EtCN. For clarity hydrogen atoms are omitted. Selected bond lengths in Å and angles in °, for closer discussion of the O–O bond length see Supporting information section 4: Cr1–O4 1.906(5), Cr1–Li1 2.705(8), Cr1–Li1’ 2.705(8), O5–Li 2.142(11), O4–O5 1.3126(10), O4-Cr-Li1’ 74.88(18), Li1-Cr-Li’ 149.8(4), O4-O5-Li1 110.3(5), O5-Li1-Cr1 65.2(2).

2 (1.334(4) Å) and rather similar to the O–O distance calculated merely for $O_2^{\cdot-}$–Na^+ (1.34 Å).[15] The coordination sphere of each sodium ion in **5**·THF is saturated by two THF molecules. A fifth THF molecule is bound to the chromium(III) center completing its octahedral coordination sphere. However, in contrast to complex **2**, in complex **5**·THF not only one alkali metal ion is lifted out of the CrO_4-plane and interacts with the superoxide ligand but both. This and the number of coordinating solvent molecules make the superoxide moiety less accessible than in the case of **2** (Supporting information Fig. S7). Consequently, the nature of the alkali metal has an influence on the M^+/O_2 interaction (Chart 1).

To determine whether the coordination of the superoxide entity (interaction with one or two alkali metal ions) is solely dependent on the alkali metal, we had a closer look at the influence the solvent has on the coordination of Li^+ to the superoxide unit in complex **2**. First tests showed that by adding nitriles to a THF solution of **2** a decrease of the absorption band at 881 nm could be observed by means of UV/vis spectroscopy (Supporting information Fig. S5), suggesting that a change of solvent also leads to a change in the superoxide/Li^+ interaction. Resonance Raman measurements performed in pure EtCN and DFT calculations corroborated the formation of a chromium(III) superoxide complex and thus – with respect to the formula – a propionitrile analogue of **2**, $[L_2Cr]Li_2O_2(EtCN)_4$ (**6**).[16] However, the change of the M^+/O_2 interaction expected based on the UV/vis results (Fig. 2 D) was confirmed by X-ray diffraction analysis performed on single crystals grown at –80 °C from a saturated propionitrile solution. The structure thus determined revealed, that the replacement of the THF solvent molecules, which coordinate to the lithium atoms in **2**, by EtCN molecules has changed the positioning of the second Li^+ ion and therefore the M^+/O_2 interaction: In the structure of **6**·EtCN both Li^+ ions are lifted out of the CrO_4 plane, so that an electrostatic interaction with the superoxide can occur from two sides like in the case of **5** (Fig. 4). In addition to this, the ligand backbone adopts a different conformation changing from a plane – as seen before in **2** and **5** – to a roof-like conformation making the superoxide moiety even more accessible than in **2** (Supporting information Fig. S7 and Fig. S8). This already quite nicely demonstrates, how small changes in the set-up e.g. the solvent or alkali metal have a major influence on the overall structure of the Cr(III) superoxide complexes.

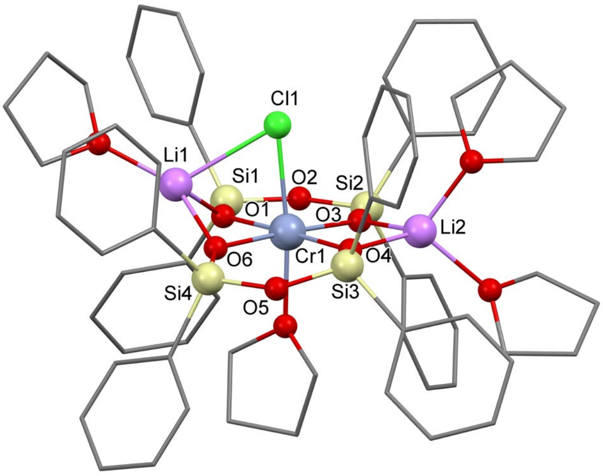

Figure 5: Molecular structure of **7**. For clarity hydrogen atoms are omitted. Selected bond lengths in Å angles in °: Cr1–O3 1.9550(13), Cr1–O6 1.9680(13), Cr1–O4 1.9711(13), Cr1–O1 1.9858(13), Cr1–Cl1 2.3655(6), Cr1–Li1 2.605(3), Cr1–Li2 2.850(3), Na1–Cl1 2.564(4), O3-Cr1-Cl1 95.02(4) ,O6-Cr1-Cl1 87.84(4),O4-Cr1-Cl1 95.41(4), O1-Cr1-Cl1 86.10(4), O6-Cr1-Li1 47.30(9), O1-Cr1-Li1 47.80(9), Cl1-Cr1-Li161.89(8), O3-Cr1-Li2 42.08(8), Cl1-Cr1-Li2 93.76(7),Li1-Cr1-Li2 155.61(10),Cr1-Cl1-Li1 63.64(8).

To ensure that the phenomena we were witnessing in the solid state – namely the structural changes within the CrO_2M_2 units depending on the alkali metal as well as the solvent – are also the ones responsible for the differing numbers of absorption bands in the UV/vis spectra recorded, we synthesized and characterized the chromium(III) chlorido complex $[L_2Cr]ClLi_2(THF)_4$ (**7**), which is temperature, light and oxygen stable. **7** can be synthesized in an analogous way to **1**, **3** and **4** by using $CrCl_3{\cdot}3THF$ as a metal precursor instead of $CrCl_2$. X-ray analysis of **7** confirmed that in **7** – as in case of **2** – one lithium ion is lifted out of the plane displaying an electrostatic interaction between the lithium ion and the axial chlorido ligand (Fig. 5).

The UV/vis spectra of **7** dissolved in THF and in the solid state both show two absorption bands at 450 nm and 780 nm (Fig. 6). This exemplifies for **7** that the structure in solution and therefore the M^+/Cl interaction is almost identical to the one adopted in the solid state and suggests for all complexes that the UV/Vis spectroscopic features reflect the environment of the chromium superoxide moiety. Hence the position of the bands not only gives us insight into what kind of oxygen adduct complex is formed but due to the absence or presence of a band in the near infrared region also indicates the type of M^+/O_2 interaction. Based on this, the topological arrangement of the product **4**+O_2 can be inferred: The existence of absorption bands at 325 nm and 725 nm corroborates the formation of a chromium superoxide with an end-on bound superoxide ligand and one THF molecule bound as an axial ligand. The absence of a band close to 500 nm suggests that the molecule is highly symmetric and therefore an even number of THF molecules (most likely four) is coordinating to the potassium ions. Finally, the absence of a band in the near infrared region suggests that the potassium ions are both interacting electrostatically with the oxygen atoms of the superoxide ligands.

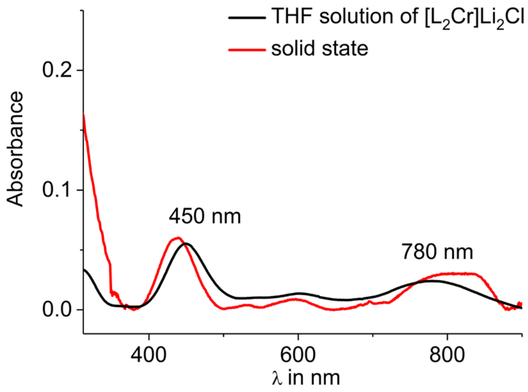

Figure 6: Absorption spectra of **7** dissolved in THF (black) and in form of a KBr pellet (red).

Influence of the alkali metal and the solvent on the stability and reactivity of the superoxide moieties In previous studies performed by Bae *et al*. on an iron peroxo complex a close correlation between the reactivity and the Lewis acidity of added metals was found.[7] However, such a clear correlation, just with the Lewis acidity, was not to be expected for the chromium superoxide series described above, as in our system due to the incorporation of the Lewis acid *into the structure*, a change in M^+ also leads to a change in the number of interactions and also to a change in the accessibility of the superoxide moieties, as clearly revealed above. To first of all evaluate the influence M^+ has on the stability of the chromium superoxide complexes the chromium(II) precursors $[L_2Cr]Li_2(THF)_4$ (**1**), $[L_2Cr]Na_2(THF)_4$ (**3**) and $[L_2Cr]K_2(THF)_4$ (**4**) were dissolved in THF or EtCN and exposed to an excess of dioxygen at 10 °C. After completion of the reaction, the decrease of the distinctive absorption bands was monitored UV/vis spectroscopically. The linear plot of the logarithmized concentration vs. time shows that the stabilities of the chromium superoxide complexes formed, decreases with decreasing Lewis acidity in the order $Li^+ > Na^+ > K^+$ in THF as well as in EtCN (see Fig. 7 for the studies with propionitrile, Supporting information Fig. S3 for THF).[17,18] This is understandable, as Li^+ as a hard Lewis acid interacts with the superoxide strongly, thus stabilizing the system more than K^+. Decay in THF and EtCN is most likely initiated by a C–H bond cleavage involving the solvent (Supporting Information 1.3.1.1).

Consequently, the question arose, whether this dependency on the Lewis acidity of the alkali metal, as observed for the stability, would also be reflected in the reactivity of these superoxide complexes towards external substrates. O–H bonds are known to be susceptible to being attacked by superoxide moieties,[19–22] and consistently complex **2** had proven capable of cleaving weak O–H bonds such as the one of TEMPO–H, as we previously reported. Therefore the reaction of $[L_2Cr]Li_2O_2$, $[L_2Cr]Na_2O_2$ and $[L_2Cr]K_2O_2$ towards weak O–H bonds was more closely investigated.

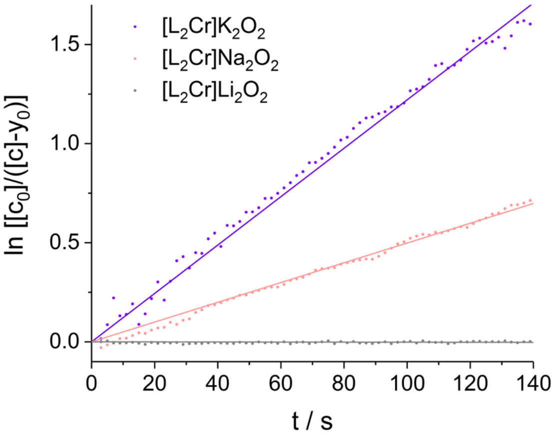

Figure 7: Self-decay rates of the *in-situ* formed superoxides monitored via UV/vis spectroscopy (2mM propionitrile solutions at 10 °C). red: **4** + O_2, black: **3** + O_2, blue: **1** + O_2 (with c = concentration of complex, c_0 = starting concentration, y_0 = correction parameter).

To compare the reactivity of the different superoxide complexes with each other, **1**, **3** and **4** were initially dissolved in THF and the solutions were then treated with an excess of dioxygen. After completion of the activation step, the respective reaction solution was purged with argon and different substrates were added. Upon addition of TEMPO–H (BDE 70.0 kcal/mol)[23] to the THF solution of the superoxides at –80 °C a decrease of the distinctive absorption bands could be observed UV/vis spectroscopically within seconds. The reaction mixtures were analyzed by means of EPR spectroscopy and the recorded data revealed the formation of a nitroxide radical confirming that all generated chromium superoxides are capable of abstracting a hydrogen atom from TEMPO–H (Supporting information Fig. S1).

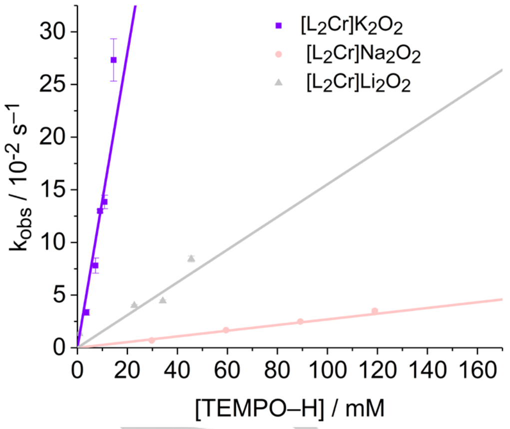

Figure 8: Plot of pseudo first-order rate constant (k_{obs}) versus the concentration of TEMPO–H to determine the second order rate constant.

A determination of second order rate constants for all complexes at –80 °C resulted in the finding that in THF the complex $[L_2Cr]K_2O_2(THF)_5$ ($k_2 = 14 \pm 0.6\ M^{-1}s^{-1}$) shows the highest reactivity, followed by $[L_2Cr]Li_2O_2(THF)_5$ (**2**) ($k_2 = 1.6 \pm 0.3\ M^{-1}s^{-1}$), with complex $[L_2Cr]Na_2O_2(THF)_5$ (**5**) ($k_2 = 0.27 \pm 0.01\ M^{-1}s^{-1}$) being the least reactive (Fig. 8). The fact that the largest rate constant was observed in the case of M = K^+ can be rationalized considering the finding that K^+ also stabilized the superoxide least.

On this basis one should have expected that **5** shows a higher reactivity than **2**. However, apparently, electronic effects are overruled here by steric effects: as pointed out above, the superoxide unit in **5** is less well accessible for a substrate than the one in **2**. That steric effects do play a role is also underlined by the results obtained changing the solvent from THF to EtCN. By using propionitrile as a solvent a drastical increase in reactivity (making the determination of rate constants for **4**-O_2 impossible) with no change in the overall trend could be observed (Supporting information 1.3.1.2), while, notably, an active participation of the solvents in the reaction mechanism – an alternative conceivable explanation[24] – could be ruled out (Supporting information section 2). When the experiments were repeated with 2,6-di-methyl-phenol (BDE 84.50 kcal/mol)[25]; which has a far stronger O–H bond, the reaction was slowed down to an extent, that an extra set of absorption bands upon addition of the substrate (Li^+ 561, 594 nm, Na^+ 507, 583 nm, K^+ 509, 574 nm) could be observed by means of UV/vis spectroscopy. These originated most likely from the coordination of the substrate to the complex close to the active center. The overall reactivity trend observed was identical to the one previously found for TEMPO–H and 3,3',5,5'-tetra-methyl-4,4'-diphenoquinone was identified as the product. When the reaction was performed with 2,6-di-*tert*-butylphenol (BDE 82.80 kcal/mol)[25], a substrate with sterically more demanding substituents in *ortho* position to the O–H bond, again the formation of the coupling product 3,3',5,5'-tetra-*tert*-butyl-4,4'-diphenoquinone (DPQ) (Scheme 2) could be observed and verified by means of GC and UV/vis spectroscopy. Remarkably, here also a change of the reactivity trend from $[L_2Cr]Na_2O_2<[L_2Cr]Li_2O_2<[L_2Cr]K_2O_2$ to $[L_2Cr]Li_2O_2<[L_2Cr]Na_2O_2<[L_2Cr]K_2O_2$ could be observed (no second order rate constants were determined for the substituted phenols, for reasons given see Supporting information 1.3.1.2). During these reactions, no coordination of the substrate close to the active center could be observed UV/vis spectroscopically. We therefore assume that due to the sterical demand of the substituents of the substrate coordination of the phenol is hindered or even prohibited, which leads to the changed reactivity trend. This meets the expectations based on the previous arguments that the reaction rates are influenced by electronic effects but with increasing bulkiness of the substrate increasingly also by the accessibility/proximity of the superoxide moiety.

10.1002/chem.201900236

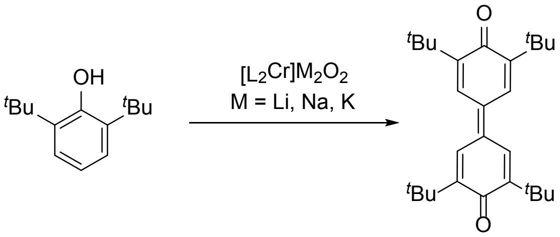

Scheme 2: Formation of 3,3',5,5'-tetra-*tert*-butyl-4,4'-dipheno-quinone.

Overall we could thus show that the reactivity is influenced by the nature of M^+ (as this determines the coordination type of M^+/O_2 and therefore the structural arrangement and accessibility of the superoxide moiety), the solvent (which influences the arrangement of the ligand and the M^+/O_2 interaction) and the bulkiness of the substrate. A closer investigation of the role the sterical demand of the ligand plays will be part of future work.

Conclusions

To summarize, we have investigated a series of chromium(II) complexes $[L_2Cr]M_2(THF)_y$ ($M^+ = Li^+$, Na^+, K^+ and y = 2, 4) with different alkali metals incorporated in their structure in combination with O_2 and studied the chromium(III) superoxides thus formed. The superoxide ligands were found to interact with M^+ in varying modes. The structure, reactivity and stability of the superoxide complexes is strongly dependent on these binding modes, on the nature inherent to the metal ions M^+ and the solvent employed. The results thus indicate that redox inactive metals can be utilized not only to stabilize reactive metal-dioxygen adducts but also to control their behavior, with the choice of solvent adding a further parameter of influence. Overall the results outline that in complexes, which have redox-inactive Lewis acids embedded in their structure, the reactivity is not solely influenced by the Lewis acidity but also by further parameters, which play an important role concerning the reactivity and thus should not be neglected. For the superoxides discussed here we could show that the accessibility of the active center is one parameter. These results thus overall contribute not only to a better understanding of dioxygen activation reactions but also add to the understanding of why a replacement/substitution of such redox-inactive metals in systems, where the Lewis acids are embedded in the structures (such as the oxygen evolving complex of photosystem II or heterogeneous catalysts), often results in a significant change of reactivity.

Experimental Section

General considerations

All manipulations were carried out in a glovebox, or by means of Schlenk-type techniques involving the use of a dry argon atmosphere. 1,1,3,3-tetraphenylsilan-1,3-diol was synthesized according to literature.[26] 1,3-dichloro-1,1,3,3-tetraphenylsiloxane, TEMPO, and $CrCl_2$ were purchased at ABCR, $CrCl_3 \cdot 3$ THF at Sigma Aldrich and used as received. 2,6-di-*tert*-butylphenol and 2,6-di-methyl-phenol were re–crystallized 5times prior to use. THF was distilled over sodium, degassed and stored over activated molecular sieves (3 Å) prior to use. Hexane was dried with an MBraun® solvent purification system and degassed prior to use. Propionitrile was purchased from Acros Organics as well as from Sigma Aldrich, degassed and stored over activated molecular sieves (3 Å) prior to use. Deuterated solvents were purchased from Eurisotop and used without further purification.

Analytical methods

Microanalyses were performed with a Leco CHNS-932 elemental analyzer. **Infrared (IR)** spectra were recorded with samples prepared as KBr pellets with a Shimadzu FTIR-8400S spectrometer. **HR-ESI-MS** data were collected using an Agilent Technologies 6210 Time-of-Flight LC-MS instrument. **UV/vis** spectra were obtained at variable temperatures in a 1 cm path length quartz cuvette using an Agilent 8453 UV-visible spectrophotometer equipped with a Unisoku USP-203-A cryostat. Solid state UV/vis spectra were recorded using a Varian Cary 100 and were measured as KBr pellets. **Crystal data** were collected at a Bruker D8 Venture diffractometer at 100 K, using Mo-Kα radiation (λ = 0.71073 Å). The structures were solved by intrinsic phasing method (SHELXT-2013) and refined by full matrix least-squares procedures based on F^2 with all measured reflections (SHELXL-2013).[27] Multi-scan absorption corrections implemented in SADABS were applied to the data.[28] Non-hydrogen atoms were refined anisotropically, except disordered phenyl-residues in complex **5** and co-crystallized and coordinated solvent molecules of complexes **5** and **6**. All hydrogen atoms were introduced at their idealized positions and refined using a riding model. CCDC 1886527 (**4'**), 1886528 (**5**), 1886529 (**6**), 1886530 (**7**) contain the supplementary crystallographic data for this paper. These data can be obtained free of charge from The Cambridge Crystallographic Data Centre via www.ccdc.cam.ac.uk/data_request/cif. **NMR spectra** were recorded with a Bruker DPX 300 for $CDCl_3$ solutions at 25 °C. The ^1H NMR spectra were calibrated against the internal residual proton of the deuterated solvents. **GC-MS** measurements were performed using a Varian 4000 GC-MS equipped with a VF-5ms Capillary Column. **Resonance Raman** spectra were recorded with a triple Raman spectrometer (Acton TriVista TR557) employing an Ar^+ ion laser with a wavelength of 496.5 nm and a power of 100 mW.

Synthesis

General procedure for preparation of 1, 3 and 4

To a solution of 1,1,3,3-tetraphenylsilan-1,3-diol (200 mg, 0.48 mmol, 1 equiv) in THF two equivalents of a) lithium-*tert*-butoxide (77.3 mg, 0.96 mmol, 2 equiv), b) sodium-*tert*-butoxide (92.7 mg, 0.96 mmol, 2 equiv), c) potassium-*tert*-butoxide (108.1 mg, 0.96 mmol, 2 equiv) were added and the solution was stirred for one hour at room temperature. After adding 0.5 equivalents $CrCl_2$ (29.6 mg, 0.24 mmol, 0.5 equiv) the resulting suspension was stirred overnight and filtered. Subsequently the solvent was removed under reduced pressure. The solid residue was washed with hexane and dried. Orange crystals of a) **1** (170 mg**,** 0.14 mmol, 60 %), b) **3** (187 mg, 0.15 mmol, 65 %), c) **4'** (197.4 mg, 0.16 mmol, 66 %) suitable for single crystal X-ray diffraction analysis were grown by layering a saturated THF solution of the product with hexane.

(**1**) HR-ESI-MS, crystal structure, IR, UV/vis data (THF) and elemental analysis in accordance with ref. 9, (**3**) crystal structure, UV/vis data in accordance with ref. 11, **IR $\tilde{\upsilon}_{max}$/cm^{-1} (KBr**): 3067(m), 3046 (m), 2997 (m), 2975 (m), 2875 (m), 1960 (w), 1894 (w), 1824 (w), 1590 (w), 1484 (w), 1428 (s), 1262 (w), 1185 (w), 1118 (s), 1049 (m), 1030 (m), 1004 (s), 988 (bs), 915 (s), 743 (m), 700 (s), 578 (m), 529 (s), 486 (m). (**4**) **IR $\tilde{\upsilon}_{max}$/cm^{-1} (KBr**): 3065 (m), 3045 (m), 2997 (m), 2975 (m), 2872 (m), 1960 (w), 1894 (w), 1824 (w), 1589 (w), 1484 (w), 1427 (s), 1262 (w), 1185 (w), 1113 (s), 1052 (m), 1030 (m), 1002 (s), 954 (bs), 912 (s), 744 (m), 701 (s), 578 (m), 525 (s), 486 (m). **UV/vis λ$_{max}$(THF)/nm (ε/cm^{-1} mol^{-1} L):** 371 (38), 462 (26). **HR-ESI-MS [M–4·THF–2K$^+$+O]$^-$**: [$C_{48}H_{40}CrO_6Si_4O$]$^-$: calcd. 893.1340, found 893.1370. As a measurement under completely inert conditions is not possible only a partially oxidized species can be detected. **Elemental analysis**, found: H 3.7, C 48.9 %, calcd. for $C_{48}H_{40}CrO_6Si_4K_2$+3·KCl: H 3.4, C 49.0 %. Due to the solubility of KCl in THF it was not possible to obtain a completely KCl free sample.

Synthesis of compound 7

To a solution of 1,1,3,3-tetraphenylsilan-1,3-diol (100 mg, 0.24 mmol, 1 equiv) in THF two equivalents of lithium-*tert*-butoxide (38.6 mg, 0.48 mmol) were added and the solution was stirred for three hours at room temperature. After adding 0.5 equivalents $CrCl_3$·3THF (44.9 mg, 0.12 mmol) the resulting green solution was stirred overnight and filtered. Subsequently the solvent was removed under reduced pressure. The green solid residue was washed with hexane and dried. Green crystals of **6** (120 mg, 0.1 mmol, 84 %) suitable for single crystal X-ray diffraction analysis were grown by layering a saturated THF solution of the product with hexane.

IR ū$_{max}$/cm^{-1} (**KBr**): 3065(m), 3046 (m), 2998 (m), 2975 (m), 2878 (m), 1960 (w), 1890 (w), 1825 (w), 1630 (w), 1590 (w), 1485 (w), 1457 (w), 1427 (s), 1261 (w), 1186 (w), 1111 (s), 1034 (s), 1013 (s), 994 (s), 967 (bs), 890 (w), 743 (m), 712 (s), 701 (s), 528 (s), 480 (w), 442 (m). **UV/vis λ$_{max}$(THF)/nm:** 450, 605, 783 nm, **UV/vis λ$_{max}$(KBr)/nm:** 438, 598, 807 nm**. HR-ESI-MS [M–4·THF–Cl]$^+$:** [$C_{48}H_{40}CrO_6Si_4Li_2$]$^+$: calcd. 890.1622, found 890.1623. **Elemental analysis** found: H 5.8, C 61.1, calcd. for $C_{64}H_{72}CrO_{10}Si_4Li_2Cl_1$+LiCl: H 5.8, C 61.2. Due to the solubility of LiCl in THF it was not possible to obtain a completely LiCl free sample.

General procedure for the preparation of 5 and 6

1 (solid) or **3** (THF solution) were exposed to dioxygen at –80 °C. The solid was dissolved in pre-cooled EtCN. Solutions of **5** and **6** were subsequently layered with pre–cooled hexane and stored at –80 °C. Crystals suitable for X-ray diffraction analysis could be isolated after 10 days. Due to the temperature and light sensitivity of the samples a determination of the yield could not be done and further analysis was limited.

(**5**)**: UV/vis λ$_{max}$(THF)/nm (ε/cm^{-1} mol^{-1} L), 0 °C:** 319 (1460), 508 (72), 712 (222). **UV/vis λ$_{max}$(EtCN)/nm (ε/cm^{-1} mol^{-1} L), 0 °C:** 309 (940), 696 (115). **HR-ESI-MS [M+1e]$^-$**: [$C_{68}H_{80}CrNa_2O_{11}{}^{18}O_2Si_4$]$^-$ calcd. 1319.3984, found 1319.2469. (**6**): **UV/vis λ$_{max}$(EtCN)/nm (ε/cm^{-1} mol^{-1} L)**, –80 °C: 306 (800), 487 (80), 685 (120). **rRaman**: $^{16}O_2$: 1130 nm.

Synthesis of TEMPO–H

TEMPO (5.02 g, 32 mmol) was dissolved in a 1:1 mixture of degassed acetone and water (70 mL). Sodium dithionite (9.5 g, 55 mmol) was added and the reaction mixture was stirred for 10 min. After removal of the acetone, the reaction mixture was extracted with dry diethylether and transferred onto dried $MgSO_4$. The solution was collected via filtration and the solvent was removed. The product (3.80 g, 24 mmol, 75 %) was purified via sublimation and stored under inert conditions at –30 °C. The product purity was analyzed by means of EPR.
Radical concentration < 1 %.

Acknowledgements

We are grateful to the Deutsche Forschungsgemeinschaft (LI 714/10-1 and “Unifying Concepts in Catalysis”) as well as the Humboldt-Universität zu Berlin for financial support.

Keywords: alkali metal • superoxide• chromium • siloxide • Lewis acids

[1] A. S. Borovik, P. J. Zinn, M. K. Zart in *Activation of Small Molecules* (Publisher: W. B. Tolman), Wiley-VCH, Weinheim, 2006.

[2] e.g. (a) M. Costas, M. P. Mehn, M. P. Jensen, L. Que, Jr., *Chem. Rev.* **2004**, *104*, 939–989. (b) C. Hess, R. W. D. Welford, P. Klinman, 2008, *Chemistry of Oxygen-Activating Enzymes*; Wiley Encyclopedia of Chemical Biology 1. (c) A. Bhagi-Damodaran, M. A. Michael, Q. Zhu, J. Reed, B. A. Sandoval, E. N. Mirts, S. Chakraborty, P. Moënne-Loccoz, Y. Zhang, Y. Lu, *Nat. Chem.* **2017**, *9*, 257–263. (d) G. Henrici-Olivé, S. Olivé, *Angew. Chem. Int. Ed.* **1974**, *13*, 29–38. (e) S. Hong, Y.-M. Lee, K. Ray, W. Nam, *Coord. Chem. Rev.* **2017**, *334*, 25–42; (f) E. S. Akturk, G. P. A. Yap K. H. Theopold, *Angew. Chem. Int. Ed.*, **2015**, *54*, 14974–14977. (g) F. Dai, G. P. A. Yap, K. H. Theopold, *J. Am. Chem. Soc.* **2013**, *135*, 16774–16776. (h) A. Noor, G. Glatz, R. Müller, M. Kaupp, S. Demeshko, R. Kempe, *Nat. Chem.* **2009**, *1*, 322–325.

[3] e.g. (a) S. Fukuzumi, Y. Morimoto, H. Kotani, P. Naumov, Y. Lee, W. Nam, *Nat. Chem.* **2010**, 756–759., (b) M. Swart, *Chem. Commun.* **2013**, *49*, 6650–6652. (c) J. Prakash, G. T. Rohde, K. K. Meier, A. J. Jasniewski, K. M. Van Heuvelen, E. Münck, L. Que, Jr., *J. Am. Chem. Soc.* **2015**, *137*, 3478–3481. (d) S. Fukuzumi, K. Ohkubo, *J. Am. Chem. Soc.* **2002**, *124*, 10270–10271. (e) R. Guilard, S. Brandès, C. Tradieux, A. Tabard, M. L’Her, C. Miry, P. Gouerec, Y. Knop, J. P. Collman, *J. Am. Chem. Soc.* **1995**, *117*, 11721–11729.(f) Y. J. Park, J. W. Ziller, A. S. Borovik, *J. Am. Chem. Soc.* **2011**, *133*, 9258–9261.(g) Y. J. Park, S. A. Cook, N. S. Sickerman, Y. Sano, J. W. Ziller, A. S. Borovik, *Chem. Sci.*, **2013**, *4*, 717–726. (h) S. Yao, Y. Xiong, M. Vogt, H. Grützmacher, C. Herwig, C. Limberg, M. Driess, *Angew. Chem. Int. Ed.* **2009**, *48*, 8107-8110.

[4] e.g. (a) J. Zhang, H. Yang, T. Sun, Z. Chen, G. Yin, *Inorg. Chem.* **2017**, *56*, 834–844. (b) I. Garcia-Bosch, R. E. Cowley, D. E. Díaz, R. L. Peterson, E. I. Solomon, K. D. Karlin, *J. Am. Chem. Soc.* **2017**, *139*, 3186–3195. (c) S. Bang, Y.-M. Lee, S. Hong, K.-B. Cho, Y. Nishida, M. S. Seo, R. Sarangi, S. Fukuzumi, W. Nam, *Nat. Chem.* **2014**, *6*, 934–940. (d) S. Hong, Y.-M. Lee, M. Sankaralingam, A. K. Vardhaman, Y. J. Park, K.-B. Cho, T. Ogura, R. Sarangi, S. Fukuzumi, W. Nam, *J. Am. Chem. Soc.* **2016**, *138*, 8523–8532.

[5] H. Yoon, Y.-M. Lee, X. Wu, K.-B. Cho, R. Sarangi, W. Nam, S. Fukuzumi, *J. Am. Chem. Soc.* **2013**, *135*, 9186–9194.

[6] S. Hong, F. F. Pfaff, E. Kwon, Y. Wang, M.-S. Seo, E. Bill, K. Ray, W. Nam, *Angew. Chem. Int. Ed.* **2014**, *53*, 10403–10407.

[7] S. H. Bae, Y-M. Lee, S. Fukuzumi, W. Nam, *Angew. Chem. Int. Ed.* **2017**, *56*, 801–805.

[8] K. Ohkubo, S. C. Menon, A. Orita, J. Otera, S. Fukuzumi, *J. Org. Chem.* **2003**, *68*, 4720–4726.

[9] F. Schax, S. Suhr, B. Braun, E. Bill, C. Herwig, C. Limberg, *Angew. Chem. Int. Ed.*, **2015**, *54*, 1352–1356.

[10] e.g. (a) K. Qin, C. D. Incarvito, A. L. Rheingold, K. H. Theopold, *Angew. Chem. Int. Ed.* **2002**, *41*, 2333–2335. (b) J. Cho, J. Woo, W. Nam, *J. Am. Chem. Soc.* **2010**, *132*, 5958–5959., (c) A. Yokoyama, J. E. Han, J. Cho, M. Kubo, T. Ogura, M. A. Siegler, K. D. Karlin, W. Nam, *J. Am. Chem. Soc.* **2012**, *134*, 15269–15272., (d) J. Cho, J. Woo, J. E. Han, M. Kubo, T. Ogura, W. Nam, *Chem. Sci.* **2011**, *2*, 2057–2062.(e) A. Yokoyama, K.-B. Cho, K. D. Karlin, W. Nam, *J. Am. Chem. Soc.* **2013**, *135*, 14900–14903. (f) M. H. Dickman, M. T. Pope, *Chem. Rev.* **1994**, *94*, 569–584.

[11] M. Motevalli, M. Sanganee, P. D. Savage, S. Shah, A. C. Sullivan, *J. Chem. Soc., Chem. Commun.* **1993**, 1132–1133.

[12] A. Kumar, D. Lionetto, V. W. Day, J. D. Blakemore, *Chem. Eur. J.* **2018**, *24*, 141–149.

[13] J. E. M. N. Klein, A. Draksharapu, A. Shokri, C. J. Cramer, L. Que, Jr., *Chem. Eur. J.* **2018**, *24*, 5373–5378.

[14] D. J. Willock in “*Molecular Symmetry*“, Wiley-VCH, Weinheim, 2009.

[15] J. M. C. Plane, B. Rajasekhar, L. Bartolotti, *J. Phys. Chem.* **1989**, *93*, 3141–3145.

[16] P. Holland, *Dalton Trans.* **2010**, *39*, 5415–5425.

[17] I. D. Brown, A. Skowron, *J. Am. Chem. Soc.* **1990**, *112*, 3401–3403.

[18] M. E. Brynildson, A. Bakac, J. H. Espenson, *J. Am. Chem. Soc.* **1987**, *109*, 4579–4583.

[19] J. Y. Lee, R. L. Peterson, K. Ohkubo, I. Garcia-Bosch, R. A. Himes, J. Woertink, C. D. Moore, E. I. Solomon, S. Fukuzumi, K. D. Karlin, *J. Am. Chem. Soc.* **2014**, *136*, 9925–9937.

[20] D.-H. Chin, G. Chiericato Jr., E. J. Nanni Jr., D. T. Sawyer, *J. Am. Chem. Soc.* **1982**, *104*, 1296–1299.

[21] S. Kim, J. Y. Lee, R. E. Cowley, J. W. Ginsbach, M. A. Siegler, E. I. Solomon, K. D. Karlin, *J. Am. Chem. Soc.* **2015**, *137*, 2796–2799.

[22] S. Fukuzumi, K. D. Karlin, *Coord. Chem. Rev.* **2013**, *257*, 187–195.

[23] J. J. Warren, T. A. Tronic, J. M. Mayer, *Chem. Rev.* **2010**, *110*, 6961–7001.

[24] T. Mallat, A. Baiker, *Catal. Sci. Technol.*, **2011**, *1*, 1572–1583.

[25] M. Lucarini, P. Pedrielli, G. F. Pedulli, S. Cabiddu, C. Fattuoni, *J. Org. Chem.*, **1996**, 9259–9263.

[26] H. Seki, Y. Abe, T. Gunji, *J. Organomet. Chem.* **2011**, *696*, 846–851.

[27] a) G. M. Sheldrick, *Acta Crystallogr. Sect A* **2008**, *64*, 112–122. b) G. M. Sheldrick, SHELXL-2013, Program for Crystal Structure Refinement, University of Göttingen, Germany, 2013.

[28] G. M. Sheldrick, SADABS, University of Göttingen, Germany, 1996.

Entry for the Table of Contents (Please choose one layout)

Layout 1:

FULL PAPER

The influence of alkali metal ions on the stability and reactivity of a chromium superoxide moiety goes beyond their electronic, Lewis acidic properties: their individual nature determines the number of contacts and the structures, which adds steric effects to reactivity.

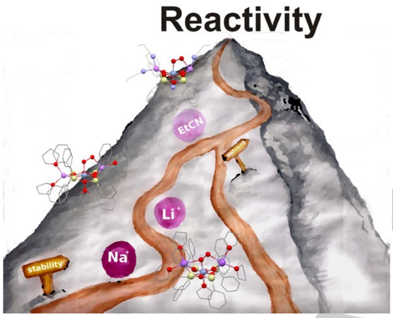

Marie-Louise Wind, Santina Hoof, Christian Herwig, Beatrice Braun-Cula and Christian Limberg*

Page No. – Page No.

The influence of alkali metal ions on the stability and reactivity of chromium(III) superoxide moieties

Layout 2:

FULL PAPER

((Insert TOC Graphic here; max. width: 11.5 cm; max. height: 2.5 cm))

*Author(s), Corresponding Author(s)**

Page No. – Page No.

Title

Text for Table of Contents